

Fundamental Studies on Induction Heating and Stirring of Non-Metallic Molten Fluid

著者	N Yoshikawa, K Watanabe, T Igarashi, S Komarov
journal or publication title	IOP Conference Series: Materials Science and Engineering
volume	424
number	012080
page range	1-5
year	2018
URL	http://hdl.handle.net/10097/00125587

doi: 10.1088/1757-899X/424/1/012080

PAPER • OPEN ACCESS

Fundamental Studies on Induction Heating and Stirring of Non-Metallic Molten Fluid

To cite this article: N. Yoshikawa *et al* 2018 *IOP Conf. Ser.: Mater. Sci. Eng.* **424** 012080

View the [article online](#) for updates and enhancements.



IOP | ebooks™

Bringing you innovative digital publishing with leading voices to create your essential collection of books in STEM research.

Start exploring the collection - download the first chapter of every title for free.

Fundamental Studies on Induction Heating and Stirring of Non-Metallic Molten Fluid

N. Yoshikawa¹, K. Watanabe², T. Igarashi² and S. Komarov¹

¹ Graduate School of Environmental Studies (GSES), Dept. of Materials Science and Engineering, Tohoku University
6-6-02, aza-Aoba, Aramaki, Aoba-ku, Sendai, Japan, 980-8579

² Graduate student at Tohoku University, GSES

Corresponding author: yoshin@tohoku.ac.jp

Abstract

Induction heating of non-metallic molten fluid has been investigated, mainly performed on melt glass stirring. Because silicate glass has relatively high viscosity and low electric conductivity for induction stirring, their experiments require very high temperature above 1500°C, and are difficult for observation and measurements. In this report, observation and simulation of heat generation and flow in molten salt are presented. And flow states of molten vanadium oxide glass is observed, both of them have low melting points. It is intended to investigate them from both experimental and theoretical directions, as a fundamental research. It is demonstrated that molten NaCl-KCl possessed the low impedance value in frequency range of hundred kHz to 1MHz, preferable for giving rise to induction current generation. Circulating flow of the fluids from the container wall to the center was observed. Temperature measurement in the melt was also conducted at various positions with respect to the coil configuration. The flow velocity and temperature distribution were analyzed by numerical simulation, and compared with the measurements, taking account of the transparent nature of the molten salts. They are shown to explain the experimental results, mostly. Molten vanadium oxide glass having the similar physical properties exhibited the similar flow characteristics.

Key words : non-metallic fluid, flow, observation, temperature distribution, electric conductivity, simulation,

Introduction

Induction heating and stirring of molten metal has been applied for melting and refining of metals, and for recycling of metal scraps etc. The flow and heat transfer analysis are one of the major subjects in this conference. Many researches have been performed so far, and contributed to promoting understanding of the processes. On the other hand, induction of heating and stirring of non-metallic fluid has been performed relatively less. One of its major purposes is a necessity of heating and stirring of glass for solidification stabilization of high-level radioactive wastes in confining in a canister, before burial in the deep undergrounds.

It is known that the silicate glass has relatively high viscosity and low electric conductivity for induction stirring even above 1500°C. Therefore, impeller stirring has been taken into consideration instead of induction stirring [1,2]. Because very high temperature experiments are required for reducing the viscosity and increasing the conductivity, relatively less experimental studies have been conducted for measurement of temperature and flow states than that by the theoretical analysis [3,4]. Besides, because the physical properties of molten glass have large temperature dependences, the flow simulation becomes more complicated, compared with that of molten metal cases.

In order to obtain a basic understanding of high frequency heating and stirring of non-metallic molten fluids, this study is intended to investigate them both from the experimental and the theoretical directions, as a fundamental study. The authors selected NaCl-KCl molten salt as an object for their analysis in the first step, because of much low viscosity and relatively high electric conductivity, comparing with silicate glasses as demonstrated in Fig. 1.

In this study, starting with impedance measurement of molten NaCl-KCl, temperature distribution and flow velocity are measured, then discussed by comparison with the simulation. In addition, it is intended to introduce our 'on going observation studies of flow states' by selecting a vanadium oxide glass, as the second step. Vanadium oxide is known to be a semi-conductor and is applied for some electric devices for special purposes, because of having relatively higher electric conductivity (Fig. 1). Vanadium oxide glass is known to possess mostly similar physical viscosity and electric conductance with that of NaCl-KCl [5], although these properties are known to be critically dependent on the valence of vanadium. A care has been undertaken by considering this stability of its physical properties, and it is to be incorporated into the simulation inputs in future studies.

Experimental

Specimens used in this study were commercially available salt (NaCl) and KCl, V₂O₅, and Na₂CO₃ powders of reagent grade, NaCl is manually mixed with KCl in a container made of silica. V₂O₅ and Na₂CO₃ were mixed, similarly. Because electric conductivity of these powder mixtures are too low to be inductively heated at room temperature,



SUS304 stainless steel bar is inductively heated (400kHz, max 3kW, RF Nestle Kanagawa, Japan), and the powder mixture were melted once in a container made of silica having inner diameter of 40mm and 50mm in depth. Then, the metal bar is removed and the melts were inductively heated.

Impedance measurement was conducted using an impedance analyzer in a frequency range between 4Hz and 5MHz.

Temperature measurement during the induction heating was conducted using a thin sheath K-type thermo couple ($\phi 0.3\text{mm}$) and a thermo-viewer (Nippon Avionics TH9100MR). In order to determine the heat transfer coefficient (h [$\text{W}/\text{m}^2/\text{K}$]), cooling curves of various positions of the melts were obtained, then fitted by one dimensional heat transfer equation. This h value was input for the boundary conditions in a numerical simulation of the heat transfer. Flow and magnetic field distribution were calculated by using a commercial software COMSOL Multiphysics ver. 5.2a. The value of heat transfer coefficient was almost interpreted as that of radiation, although the detailed analysis is not described in this report.

Results and Discussion

1. Measurement of electric conductivity of molten NaCl-KCl

Platinum plate electrodes were immersed in NaCl-50mol%KCl melt and impedance of the melt was measured with variation of temperature and frequency. The result of the impedance measurement is plotted in Fig. 2. It was shown that the impedance decreases as an increase of temperature and that the impedance (resistivity) become lower above 10kHz, having a minimum around hundred kHz to MHz. This result convinced us a validity of selecting the induction frequency of 400kHz for the present study.

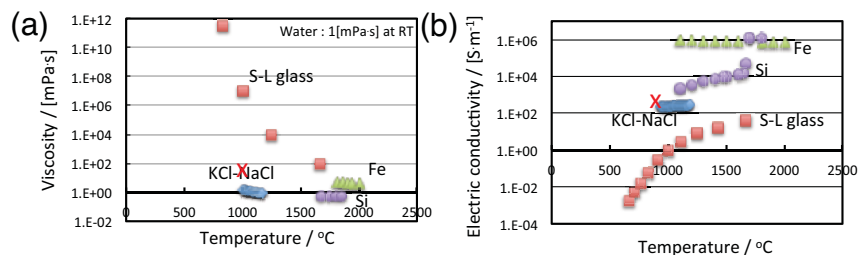


Fig. 1: Temperature dependence of (a) viscosity and (b) electric conductivity of various melts. Vanadium oxide glass values are indicated with keys of x.

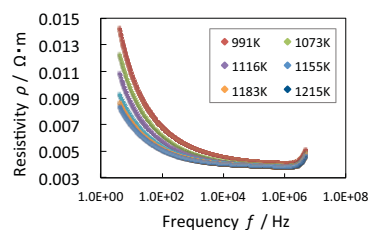


Fig. 2: Frequency dependence of NaCl-50%KCl melt impedance (resistivity), with variation of temperature.

2. Temperature measurement

After NaCl-KCl was completely melted by induction heating of stainless steel bar, (immersed in the powder mixture in advance). The melt was inductively heated, as the photos shown in Fig. 3, where states of heating change obviously, as the increase of induction voltage or the input power. The relationship between the input power and the temperature is plotted in Fig. 4. The melt container is placed in a water cooling coil, and the configuration is shown in Fig. 5.



Fig. 3: Sketch of the casting flow problem with magnet pole faces and numerical grid for the simulations.

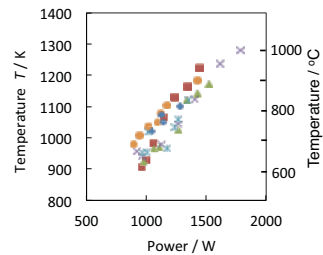


Fig. 4: Relationship between the induction power and the temperature of NaCl-KCl melt. Different marks correspond to the measurement trials.

Temperature distribution in the melt was measured with a thermo-couple and a thermo-viewer. They are demonstrated in Fig. 6. It was shown the bottom temperature is higher because of thermal insulation. Measurement of the temperature in the middle depth was not possible because of fluctuation, probably due to the flow. One of the finding is that the temperature value by thermo-viewer (*mark) is higher than that of bottom and the surface in the case of larger mass (having the large depth, (a2 in Fig. 5)). This discrepancy might be caused by an occurrence of highest temperature positioned between them. The measured value by thermo-viewer might be due to the wave length of light transmitted through the transparent melt. The radiation heat transfer in the transparent material is one of the problems to be taken into consideration for the analysis of temperature distributions in an inductively heated melts. Further study is being carried out.

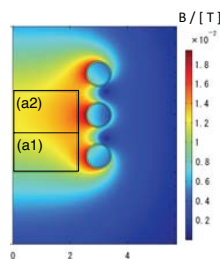


Fig. 5: Configuration of NaCl-KCl melt in the induction coil (height of 35 and 70g specimen corresponds to rectangles (a1) and (a2)), and the calculated distribution of magnetic flux density (coil current 300A).

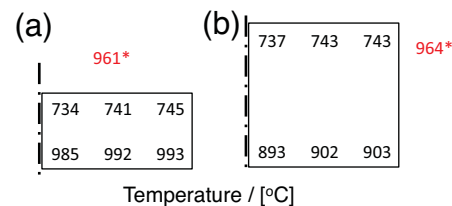


Fig. 6: Measured temperature values with a thermocouple and with a thermo-viewer, shown within and out of the rectangles (with an asterisk), corresponding to the quantity of the melts (a1, a2 in Fig. 5), respectively.

3. Induction stirring of molten NaCl-KCl and vanadium oxide glass

Flow of the NaCl-KCl melt driven by induction and its flow pattern was observed by tracer particles as a photograph shown in Fig. 7. It was demonstrated that circulating flow having down stream in the central position of the container existed. The flow state of NaCl-KCl is not clear in Fig. 7 (hence the flow directions are schematically indicated with arrows.). However, it was much easier in observation of flow pattern in vanadium oxide glass melt cases (without tracer particles), as shown in Fig. 8. The similar flow pattern is observed, because the physical properties of the melt are almost similar, as demonstrated in Fig. 1.



Fig. 7: Photograph of inductively stirred NaCl-KCl melt.



Fig. 8: Photograph of inductively stirred vanadium oxide melt.

4. Numerical simulation

In order to simulate the measured temperature and the observed flow velocity distributions in the NaCl-KCl melt, numerical simulation was performed. The software solved the equation for the magnetic field distribution (magnetic flux density \mathbf{B} [T]) expressed by Eq. 1. The induction current (\mathbf{J} [A/m²]) and the Lorentz force (\mathbf{f} [N/m³]) exerting to the melt is expressed by Eq. 2. The analysis of electromagnetic field is done in terms of vector potential (\mathbf{A}) in the software. The Lorentz force \mathbf{f} is incorporated into the Navier-Stokes equation expressed in Eq. 3 as a force term. And the induction current \mathbf{J} is also incorporated into the heat transfer equation expressed in Eq. 4 as a heat source term. The electromagnetic analysis and the flow/heat transfer analysis are assumed not mutually coupled. The output of the former is input into the latter calculation. But the flow and heat transfer equations (Eq. 3 and 4) are mutually coupled. The Parameters appeared in Eq. 1 are as follows: $\mathbf{B} = \mu\mathbf{H}$, \mathbf{H} is a magnetic field [A/m], μ is a magnetic permeability [H/m], \mathbf{E} is an electric field [V/m]. The other parameters t , \mathbf{v} , σ , p , ρ , η and g are the time [s], velocity vector [m/s], electric conductivity [S/m], pressure [Pa], density [kg/m³], viscosity [Pa·s] and gravity acceleration [m/s²], respectively.

$$\frac{\partial \mathbf{B}}{\partial t} = \nabla \times (\mathbf{v} \times \mathbf{B}) + \frac{\nabla^2 \mathbf{B}}{\sigma \mu_m} \quad (1)$$

$$\mathbf{f} = \mathbf{J} \times \mathbf{B}, \quad \mathbf{J} = \sigma(\mathbf{E} + \mathbf{v} \times \mathbf{B}) \quad (2)$$

$$\rho \left(\frac{\partial \mathbf{v}}{\partial t} + (\mathbf{v} \cdot \nabla) \mathbf{v} \right) = \eta \nabla^2 \mathbf{v} - \nabla p + \mathbf{f} + \rho \mathbf{g} \quad (3)$$

$$\rho C_p \left(\frac{\partial T}{\partial t} + \mathbf{v} \cdot \nabla T \right) = \lambda \nabla^2 T + \frac{\mathbf{J}^2}{2\sigma} \quad (4)$$

Boundary conditions used for heat and flow simulations are shown in Fig. 9. The upper surface and right side surface (S1) are cooled (as the heat transfer coefficient (h) provided as the boundary condition) and thermal insulation condition imposed at the bottom. As can be seen in Fig. 5, a magnetic field (magnetic flux density \mathbf{B}) is distributed around the coil, and \mathbf{B} is penetrated deepest into the specimen at the height of the center coil. This distribution influenced the position of heating source and the temperature distribution in the melt.

Fig. 10 demonstrates the simulated temperature distribution, corresponding to the specimen configuration shown in Fig. 5. It can be seen that the highest temperature region appears in the upper internal area a bit from the right edge (S1), which is close to the center coil. As the distance (r) from the coil increases, the heat source intensity becomes small, thus the symmetrical axis (left side (S2) in left side, adiabatic boundary condition) area has low temperature. The calculated temperature distribution looks mostly agree with the tendency of measured temperature distribution. In Fig. 10, the calculated flow velocity is also indicated. The flow patterns are consistent with the observation, as shown in Fig. 7, 8. The flow velocity on the melt surface was measured from the movie taken at the experiments. The flow pattern and the flow rate almost agreed with the simulation results, as well.

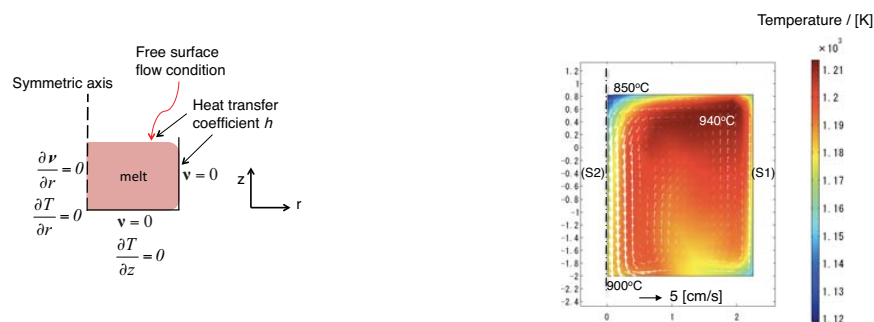


Fig. 9: Boundary conditions used for numerical simulation of flow and heat transfer in NaCl-KCl melt.

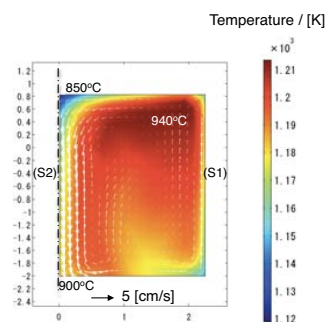


Fig. 10 : Calculated temperature and velocity distribution in NaCl-KCl melt (coil current 300A).

Conclusion

The induction heating and stirring states of NaCl-KCl and vanadium oxide glass melts were observed. Temperature measurement of the molten salt was conducted. Numerical simulation of electromagnetic and heat transfer analysis was performed for the molten salt, and the calculated distributions of magnetic field, temperature and flow velocity were presented. The calculated distributions of temperature, flow pattern and the flow velocity were almost able to explain the measurements and observation of molten salt. The observed flow pattern of vanadium oxide glass (having the similar physical properties) was similar to that of the molten salt.

References

1. S.Gopalakrishnan and A.Tess, *Int. J. Therm. Sci.*, **60** (2012) 142-152.
2. L.Jacout, Y.Fautrelle, A.Gagnound, P.Brun and J.Lacombe, *Chem. Eng. Sci.*, **63** (2008) 2391-2401.
3. B.Nacke, M.Kudryash, T.Behrens, B.Niemann, D.Lopukh, A.Martynov and S.Chepluk, *Int. Sci. Colloq. Modelling for Material Processing*, Riga, (2006) 209-214.
4. B.Nacke, V.Kichigin, V.Geza and I.Poznyak, *Proc. 8th Int. Conf. of EPM*, (2015), p.11-14.
5. V.Danek, I.Votava, K.Matiasovsky and J.Balajka, *Chem. zvesti*, **28** (1974) 728-732.